Acta Cryst E CRYSTALLOGRAPHIC COMMUNICATIONS

ISSN 2056-9890

Crystal structure, Hirshfeld surface analysis and DFT studies of (*E*)-2-{[(3-chloro-4-methylphenyl)-imino]methyl}-4-methylphenol

Md. Serajul Haque Faizi,[a] Emine Berrin Cinar,[b] Alev Sema Aydin,[b] Erbil Agar,[c] Necmi Dege[b] and Ashraf Mashrai[d]*

[a]PG Department of Chemistry, Langat Singh College, B. R. A. Bihar University, Muzaffarpur, Bihar 842001, India, [b]Ondokuz Mayıs University, Faculty of Arts and Sciences, Department of Physics, 55139, Samsun, Turkey, [c]Ondokuz Mayıs University, Faculty of Arts and Sciences, Department of Chemistry, 55139, Samsun, Turkey, and [d]Department of Pharmacy, University of Science and Technology, Ibb Branch, Ibb, Yemen. *Correspondence e-mail: ashraf.yemen7@gmail.com

Received 22 June 2020
Accepted 9 July 2020

Edited by L. Van Meervelt, Katholieke Universiteit Leuven, Belgium

Keywords: crystal structure; 3-chloro-4-methylaniline; 2-hydroxy-5-methylbenzaldehyde; Schiff base.

CCDC reference: 2015356

Supporting information: this article has supporting information at journals.iucr.org/e

The title compound, $C_{15}H_{14}ClNO$, was synthesized by condensation reaction of 2-hydroxy-5-methylbenzaldehyde and 3-chloro-4-methylaniline, and crystallizes in the monoclinic space group $P2_1/c$. The 3-chlorobenzene ring is inclined to the phenol ring by 9.38 (11)°. The configuration about the C=N bond is *E* and an intramolecular O—H···N hydrogen bond forms an *S*(6) ring motif. The Hirshfeld surface analysis of the crystal structure indicates that the most important contributions for the packing arrangement are from H···H (43.8%) and C···H/H···C (26.7%) interactions. The density functional theory (DFT) optimized structure at the B3LYP/ 6–311 G(d,p) level is compared with the experimentally determined molecular structure and the HOMO–LUMO energy gap is provided.

1. Chemical context

Schiff bases contain the azomethine moiety (–*R*CH=N–*R*′) and are prepared by condensation reactions between amines and active carbonyl compounds. Schiff bases are employed as catalyst carriers (Grigoras *et al.*, 2001), thermo-stable materials (Vančo *et al.*, 2004), metal–cation complexing agents and in biological systems (Taggi *et al.*, 2002). Schiff bases show biological activities including antibacterial, antifungal, anticancer, antiviral and herbicidal activities (Desai *et al.*, 2001; Singh & Dash, 1988; Karia & Parsania, 1999; Siddiqui *et al.*, 2006). Moreover, Schiff base ligands are potentially capable of forming stable complexes by coordination of metal ions with their nitrogen atoms as donors (Ebrahimipour *et al.*, 2012). They are important for their photochromic properties and have applications in various fields such as the measurement and control of radiation intensities in imaging systems, optical computers, electronics, optoelectronics and photonics (Iwan *et al.*, 2007). The present work is a part of an ongoing structural study of Schiff bases and their utilization in the synthesis of quinoxaline derivatives (Faizi *et al.*, 2018), fluorescence sensors (Faizi *et al.*, 2016; Mukherjee *et al.*, 2018; Kumar *et al.*, 2017, 2018) and non-linear optical properties (Faizi *et al.*, 2020). We report herein on the synthesis (from 2-hydroxy-5-methylbenzaldehyde and 3-chloro-4-methylaniline), crystal structure, Hirshfeld surface analysis and DFT computational calculations of the title compound, (I). The results of calculations by density functional theory (DFT) carried out at the

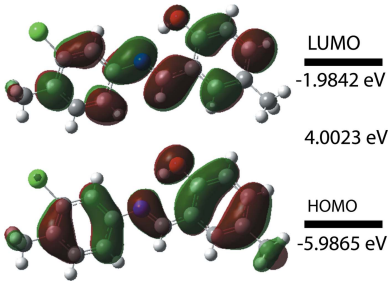

B3LYP/6–311 G(d,p) level are compared with the experimentally determined molecular structure in the solid state.

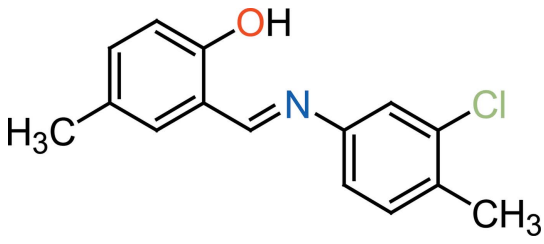

2. Structural commentary

The molecular structure of the title compound (I) is shown in Fig. 1. An intramolecular O—H···N hydrogen bond is observed (Table 1 and Fig. 1). This is a relatively common feature in analogous imine–phenol compounds (see *Database survey* section). The imine group, which displays a C9—C8—N1—C5 torsion angle of −177.49 (18)°, contributes to the general non-planarity of the molecule. The chlorobenzene ring (C2–C7) is inclined by 9.38 (11)° to the phenol ring (C9–C14). The configuration of the C7=N1 bond of this Schiff base is *E*, and the intramolecular O1—H1···N1 hydrogen bond forms an *S*(6) ring motif (Fig. 1*a* and Table 1). The C14—O1 distance [1.354 (2) Å] is close to normal values reported for single C—O bonds in phenols and salicylideneamines (Ozeryanskii *et al.*, 2006). The N1—C8 bond is short at 1.281 (3) Å, indicating the existence of an imine bond, while the long C8—C9 bond [1.446 (3) Å] implies a single bond. All these data support the existence of the phenol–imine tautomer for (I) in its crystalline state. These features are similar to those observed in related 4-dimethylamino-*N*-salicylideneanilines (Wozniak *et al.*, 1995; Pizzala *et al.*, 2000). The C—N, C=N and C—C bond lengths are normal and close to the values observed in related structures (Faizi *et al.*, 2017).

3. Supramolecular features

In the crystal packing of (I), the molecules are linked by C1—H1*A*···N1 [H1*A*···N1(−*x* + 1, −*y* + 1, −*z* + 1) = 2.86 Å] interactions, forming sheets propagating along the *a*-axis direction (Fig. 2*a*). Weak C—H···*π* interactions [C1—H1*C*···*Cg*1(−*x*, −*y* + 2, −*z*) = 2.92 Å] are observed (Table 1 and Fig. 2*b*). Notably, weak *π*–*π* stacking interactions between chlorobenzene rings [*Cg*1···*Cg*1(−*x* + 1, −*y* + 1, −*z* + 1) = 3.7890 (2) Å, where *Cg*1 is the centroid of the C2–C7 ring] along the *a* axis lead to the formation of a three-dimensional network.

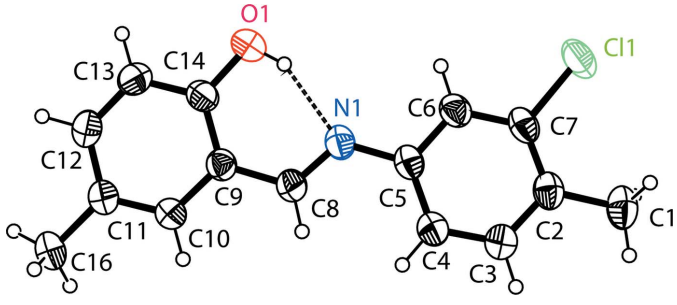

Figure 1
The molecular structure of the title compound (I), showing the atom labelling and the intermolecular O—H···N hydrogen bond as a dashed line. Displacement ellipsoids are drawn at the 40% probability level.

Table 1
Hydrogen-bond geometry (Å, °).

*Cg*1 is the centroid of the C2–C7 ring.

D—H···*A*	*D*—H	H···*A*	*D*···*A*	*D*—H···*A*
O1—H1···N1	0.79 (4)	1.89 (3)	2.625 (3)	153 (3)
C1—H1*C*···Cl1	0.96	2.91	3.072 (3)	91
C1—H1*A*···N1^{i}	0.96	2.86	3.734 (3)	152
C1—H1*C*···*Cg*1^{ii}	0.96	2.92	3.617 (2)	131

Symmetry codes: (i) $-x+1, -y+1, -z+1$; (ii) $-x, -y+2, -z$.

4. Hirshfeld surface analysis

The intermolecular interactions were investigated quantitatively and visualized with *Crystal Explorer 17.5* (Turner *et al.*, 2017; Spackman *et al.*, 2009). The shorter and longer contacts are indicated as red and blue spots, respectively, on the Hirshfeld surfaces, and contacts with distances approximately equal to the sum of the van der Waals radii are represented as white spots. The d_{norm} (*a*–*d*) and shape index (*e*) surface mappings are shown in Fig. 3. The most important red spots on the d_{norm} surface represent O1···Cl1 interactions (Fig. 3*b*) and C1—H1*C*···*Cg*1 interactions (Fig. 3*c*). Some additional interactions indicated by light-red spots are corresponding to contacts around phenolic and chlorobenzene rings (Fig. 3*d*). The red and blue triangles are absent on the shape-index surface, which indicates there are no strong *π*–*π* stacking interactions in the crystal structure.

Analysis of the two-dimensional fingerprint plots (Fig. 4*a*–*f*) indicates that the H···H (43.8%) interactions are the major factor in the crystal packing with C···H/H···C (26.7%)

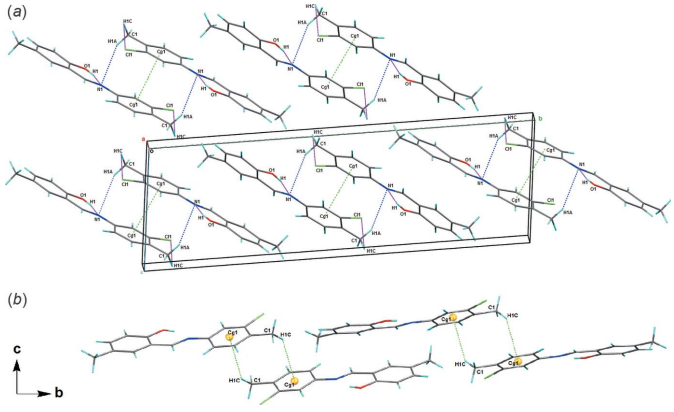

Figure 2
A view along the *a* axis of the crystal packing of title compound (I) showing (*a*) the C1—H1*C*···*Cg*1 interactions and (*b*) the most important interactions as dashed lines.

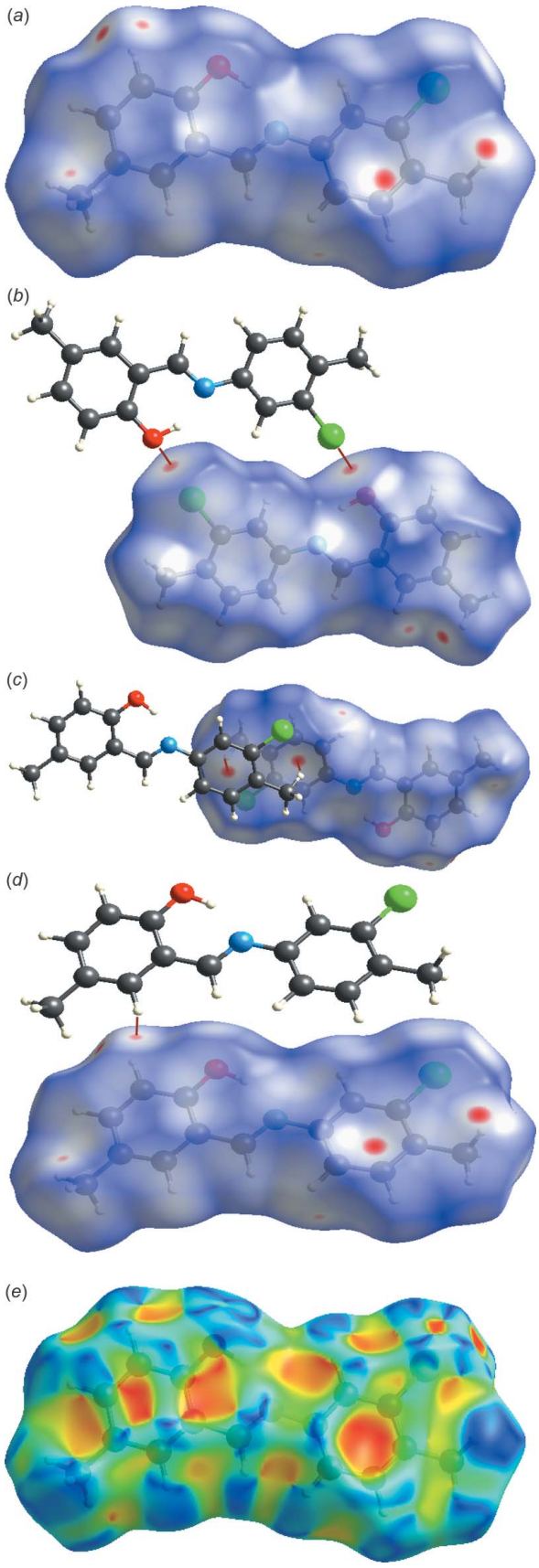

Figure 3
A view of the three-dimensional Hirshfeld surface for (I), plotted over (*a*)–(*d*) d_{norm} and (*e*) shape-index.

interactions making the next highest contribution. The percentage contributions of other weak interactions are: Cl···H/H···Cl (12.4%), O···H/H···O (6.6%) and N···H/H···N (3.8%).

5. DFT calculations

The optimized structure in the gas phase of compound (I) was generated theoretically *via* density functional theory (DFT) using standard B3LYP functional and 6–311 G(d,p) basis-set calculations (Becke, 1993) as implemented in *GAUSSIAN 09* (Frisch *et al.*, 2009). The theoretical and experimental results are in good agreement (Table 2). The highest-occupied molecular orbital (HOMO), acting as an electron donor, and the lowest-unoccupied molecular orbital (LUMO), acting as an electron acceptor, are very important parameters for quantum chemistry. When the energy gap is small, the molecule is highly polarizable and has high chemical reactivity (Fukui, 1982; Khan *et al.*, 2015). The DFT calculations provide some important information on the reactivity and site selectivity of

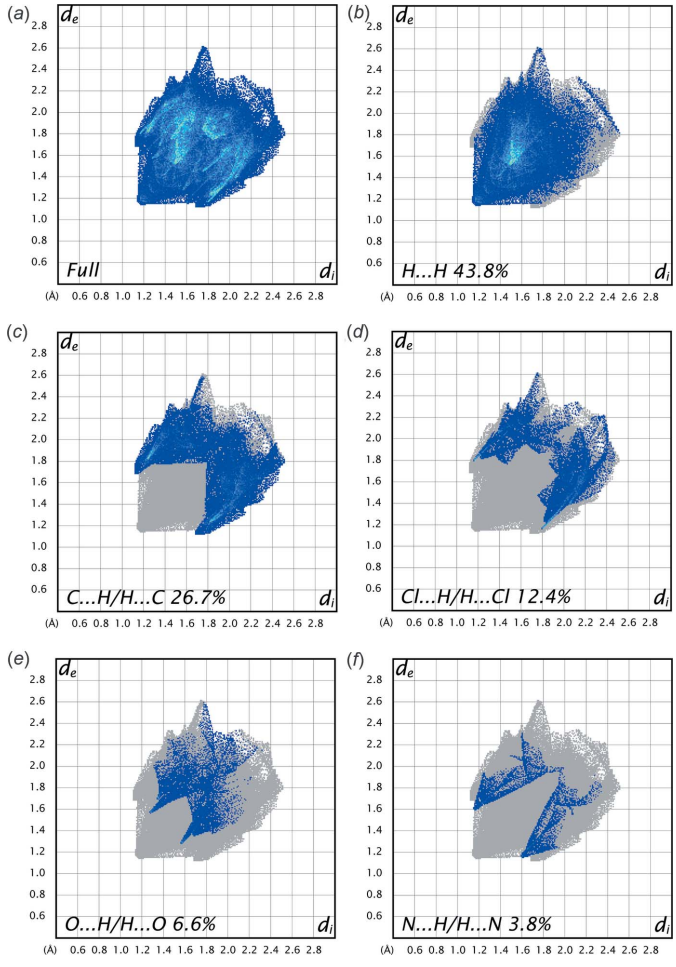

Figure 4
(*a*) The overall two-dimensional fingerprint plot for the title compound and (*b*)–(*f*) those delineated into H···H, C···H/H···C, Cl···H/H···Cl, O···H/H···O and N···H/H···N contacts, respectively.

Table 2
Comparison of observed (X-ray data) and calculated (DFT) geometric parameters (Å, °).

Parameter	X-ray	B3LYP/6–311G(d,p)
O1—C14	1.354 (2)	1.354
C7—Cl1	1.735 (2)	1.735
N1—C8	1.281 (3)	1.281
C8—C9	1.446 (3)	1.446
N1—C5	1.418 (3)	1.418
C2—C7	1.385 (3)	1.385
C13—C14—C9	119.36 (19)	119.4
C9—C8—N1	121.82 (19)	121.8
C8—N1—C5	122.08 (19)	122.1

the molecular framework, E_{HOMO} and E_{LUMO}, which clarify the inevitable charge-exchange collaboration inside the studied material, electronegativity (χ), hardness (η), electrophilicity (ω), softness (σ) and fraction of electron transferred (ΔN). These data are recorded in Table 3. The significance of η and σ is for the evaluation of both the reactivity and stability. The electron transition from the HOMO to the LUMO energy level is shown in Fig. 5. The HOMO and LUMO are localized in the plane extending from the whole 2-{[(3-chloro-4-methylphenyl)imino]methyl}-4-methylphenol ring. The energy band gap [$\Delta E = E_{LUMO} - E_{HOMO}$] of the molecule is 4.0023 eV, the frontier molecular orbital energies E_{HOMO} and E_{LUMO} being −5.9865 eV and −1.9842 eV, respectively. The dipole moment of (I) is estimated to be 4.30 Debye.

6. Database survey

A search of the Cambridge Structural Database (CSD, version 5.39; Groom *et al.*, 2016) gave 13 hits for the 2-{[(3-chloro-4-methylphenyl)imino]methyl}-4-methylphenol moiety. Out of 13, only a few are very closely related to the title compound. In (*E*)-4-methoxy-2-{[(4-methylphenyl)imino]methyl}phenol (DUPGOL; Koşar *et al.*, 2010), the methyl group is replaced by a methoxy group and the dihedral angle between the benzene rings is 5.46 (2)°. In 2-[(*E*)-(5-chloro-2-methylphenyl)iminomethyl]-4-methylphenol (AFILAE; Zheng, 2013), the dihedral angle between the planes of the chlorophenyl and methylphenol rings is 35.0 (3)°. In 2-{(*E*)-[(3-chloro-4-methylphenyl)imino]methyl}-4-(trifluoromethoxy)phenol (TERTUI; Atalay *et al.*, 2017), the dihedral angle between the benzene rings is 8.3 (2)° and an intramolecular O—H···N hydrogen bond closes an *S*(6) ring. In 2-{(*E*)-[(3-iodo-4-methylphenyl)imino]methyl}-4-(trifluoromethoxy)phenol (XEBCOY; Pekdemir *et al.*, 2012), the dihedral angle between the two benzene rings is 12.4 (2)°. For 4-[(2-hydroxy-5-methoxybenzylidene)amino]benzonitrile (XIGNEI; Chiang *et al.*, 2013), a complex with zinc is reported. In *N*-(5-hydroxysalicylidene)-2,4,6-trimethylaniline (ZIKNOW; Tenon *et al.*, 1995), the angle between the planes of the benzene rings is 74.5 (1)° and chlorine is absent.

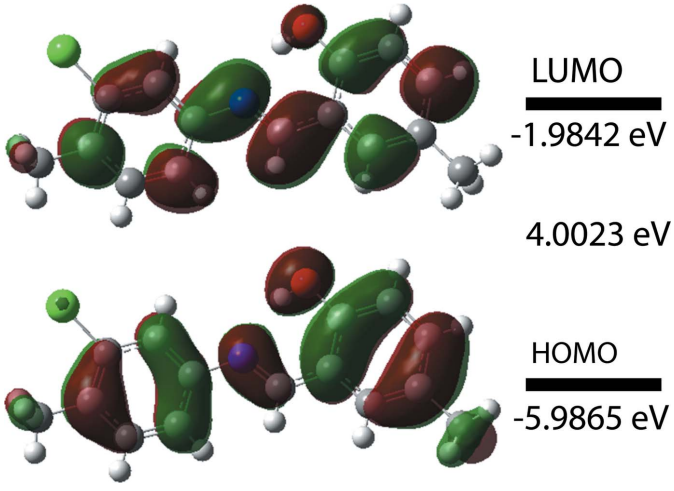

Figure 5
Molecular orbitals showing the HOMO–LUMO electronic transition in the title compound.

Table 3
Calculated molecular energies for (I).

Molecular Energy (a.u.) (eV)	Compound (I)
Total Energy *TE* (eV)	−31841.0844
E_{HOMO} (eV)	−5.9865
E_{LUMO} (eV)	−1.9842
Gap, ΔE (eV)	4.0023
Dipole moment, μ (Debye)	4.30
Ionization potential, I (eV)	5.9865
Electron affinity, A	1.9842
Electronegativity, χ	3.985
Hardness, η	2.001
Electrophilicity index, ω	3.968
Softness, σ	0.250
Fraction of electron transferred, ΔN	0.754

7. Synthesis and crystallization

The title compound was prepared by refluxing mixed solutions of 2-hydroxy-5-methylbenzaldehyde (34.0 mg, 0.25 mmol) in ethanol (15 ml) and 3-chloro-4-methylaniline (35.4 mg, 0.25 mmol) in ethanol (15 ml). The reaction mixture was stirred for 5 h under reflux. Single crystals of the title compound suitable for X-ray analysis were obtained by slow evaporation of an ethanol solution (yield 65%, m.p. 383–386 K).

8. Refinement

Crystal data, data collection and structure refinement details are summarized in Table 4. The hydroxy *H* atom was located in a difference-Fourier map and its positional parameters were refined freely with $U_{iso}(H) = 1.5U_{eq}(O)$. Other H atoms were fixed geometrically and treated as riding with C—H = 0.96 Å (methyl) or 0.93 Å (aromatic), and $U_{iso}(H) = 1.2U_{eq}(C)$ for aromatic *H* atoms or $U_{iso}(H) = 1.5U_{eq}(C)$ for methyl H atoms.

Acknowledgements

Langat Singh College, B. R. Bihar University India, is thanked for the use of laboratory facilities.

Table 4
Experimental details.

Crystal data	
Chemical formula	$C_{15}H_{14}ClNO$
M_r	259.72
Crystal system, space group	Monoclinic, $P2_1/c$
Temperature (K)	296
a, b, c (Å)	8.0534 (5), 6.3764 (3), 25.3657 (16)
β (°)	96.392 (5)
V (Å^3)	1294.47 (13)
Z	4
Radiation type	Mo $K\alpha$
μ (mm^{-1})	0.28
Crystal size (mm)	0.65 × 0.37 × 0.21
Data collection	
Diffractometer	Stoe IPDS 2
Absorption correction	Integration (*X-RED32*; Stoe & Cie, 2002)
T_{min}, T_{max}	0.885, 0.958
No. of measured, independent and observed [$I > 2\sigma(I)$] reflections	7752, 2414, 1801
R_{int}	0.040
(sin $\theta/\lambda)_{max}$ (Å^{-1})	0.606
Refinement	
$R[F^2 > 2\sigma(F^2)]$, $wR(F^2)$, S	0.045, 0.137, 1.03
No. of reflections	2414
No. of parameters	169
H-atom treatment	H atoms treated by a mixture of independent and constrained refinement
$\Delta\rho_{max}$, $\Delta\rho_{min}$ (e Å^{-3})	0.22, −0.26

Computer programs: *X-AREA* and *X-SHAPE* (Stoe & Cie, 2002), *SHELXT2018/2* (Sheldrick, 2015*a*), *SHELXL2018/3* (Sheldrick, 2015*b*), *ORTEP-3 for Windows* (Farrugia, 2012) and *XP* in *SHELXTL* (Sheldrick, 2008).

Funding information

This study was supported financially by Université Sidi Mohamed Ben Abdallah, Faculté des Sciences et Techniques, Morocco, the University of Science and Technology, Ibb Branch, Ibb, Yemen, and a start-up grant from the University Grants Commission (UGC).

References

Atalay, Ş., Gerçeker, S., Meral, S. & Bülbül, H. (2017). *IUCrData*, **2**, x171725.
Becke, A. D. (1993). *J. Chem. Phys.* **98**, 5648–5652.
Chiang, H.-W., Su, Y.-T. & Wu, J.-Y. (2013). *Dalton Trans.* **42**, 15169–15182.
Desai, S. B., Desai, P. B. & Desai, K. R. (2001). *Heterocycl. Commun.* **7**, 83–90.
Ebrahimipour, S. Y., Mague, J. T., Akbari, A. & Takjoo, R. (2012). *J. Mol. Struct.* **1028**, 148–155.
Faizi, M. S. H., Ahmad, M., Kapshuk, A. A. & Golenya, I. A. (2017). *Acta Cryst.* E**73**, 38–40.
Faizi, M. S. H., Alam, M. J., Haque, A., Ahmad, S., Shahid, M. & Ahmad, M. (2018). *J. Mol. Struct.* **1156**, 457–464.
Faizi, M. S. H., Gupta, S., Mohan, V. K., Jain, K. V. & Sen, P. (2016). *Sens. Actuators B Chem.* **222**, 15–20.
Faizi, M. S. H., Osório, F. A. P. & Valverde, C. (2020). *J. Mol. Struct.* **1210**, 128039–464.
Farrugia, L. J. (2012). *J. Appl. Cryst.* **45**, 849–854.
Frisch, M. J., Trucks, G. W., Schlegel, H. B., Scuseria, G. E., Robb, M. A., Cheeseman, J. R., Scalmani, G., Barone, V., Mennucci, B., Petersson, G. A., Nakatsuji, H., Caricato, M., Li, X., Hratchian, H. P., Izmaylov, A. F., Bloino, J., Zheng, G., Sonnenberg, J. L., Hada, M., Ehara, M., Toyota, K., Fukuda, R., Hasegawa, J., Ishida, M., Nakajima, T., Honda, Y., Kitao, O., Nakai, H., Vreven, T., Montgomery, J. A. Jr, Peralta, J. E., Ogliaro, F., Bearpark, M., Heyd, J. J., Brothers, E., Kudin, K. N., Staroverov, V. N., Kobayashi, R., Normand, J., Raghavachari, K., Rendell, A., Burant, J. C., Iyengar, S. S., Tomasi, J., Cossi, M., Rega, N., Millam, J. M., Klene, M., Knox, J. E., Cross, J. B., Bakken, V., Adamo, C., Jaramillo, J., Gomperts, R., Stratmann, R. E., Yazyev, O., Austin, A. J., Cammi, R., Pomelli, C., Ochterski, J. W., Martin, R. L., Morokuma, K., Zakrzewski, V. G., Voth, G. A., Salvador, P., Dannenberg, J. J., Dapprich, S., Daniels, A. D., Farkas, Ö., Foresman, J. B., Ortiz, J. V., Cioslowski, J. & Fox, D. J. (2009). *GAUSSIAN 09*. Gaussian Inc., Wallingford, CT, USA.
Fukui, K. (1982). *Science*, **218**, 747–754.
Grigoras, M., Catanescu, O. & Simonescu, C. I. (2001). *Rev. Roum. Chim.* **46**, 927–939.
Groom, C. R., Bruno, I. J., Lightfoot, M. P. & Ward, S. C. (2016). *Acta Cryst.* B**72**, 171–179.
Iwan, A., Kaczmarczyk, B., Janeczek, H., Sek, D. & Ostrowski, S. (2007). *Spectrochim. Acta A Mol. Biomol. Spectrosc.* **66**, 1030–1041.
Karia, F. D. & Parsania, P. H. (1999). *Asian J. Chem.* **11**, 991–995.
Khan, E., Shukla, A., Srivastava, A., Shweta, P. & Tandon, P. (2015). *New J. Chem.* **39**, 9800–9812.
Koşar, B., Özek, A., Albayrak, Ç. & Büyükgüngör, O. (2010). *Acta Cryst.* E**66**, o469.
Kumar, M., Kumar, A., Faizi, M. S. H., Kumar, S., Singh, M. K., Sahu, S. K., Kishor, S. & John, R. P. (2018). *Sens. Actuators B Chem.* **260**, 888–899.
Kumar, S., Hansda, A., Chandra, A., Kumar, A., Kumar, M., Sithambaresan, M., Faizi, M. S. H., Kumar, V. & John, R. P. (2017). *Polyhedron*, **134**, 11–21.
Mukherjee, P., Das, A., Faizi, M. S. H. & Sen, P. (2018). *Chemistry Select*, **3**, 3787–3796.
Ozeryanskii, V. A., Pozharskii, A. F., Schilf, W., Kamieński, B., Sawka-Dobrowolska, W., Sobczyk, L. & Grech, E. (2006). *Eur. J. Org. Chem.* pp. 782–790.
Pekdemir, M., Işık, Ş. & Alaman Ağar, A. (2012). *Acta Cryst.* E**68**, o2148.
Pizzala, H., Carles, M., Stone, W. E. E. & Thevand, A. (2000). *J. Chem. Soc. Perkin Trans. 2*, pp. 935–939.
Sheldrick, G. M. (2008). *Acta Cryst.* A**64**, 112–122.
Sheldrick, G. M. (2015*a*). *Acta Cryst.* A**71**, 3–8.
Sheldrick, G. M. (2015*b*). *Acta Cryst.* C**71**, 3–8.
Siddiqui, J. I., Iqbal, A., Ahmad, S. & Weaver, W. (2006). *Molecules*, **11**, 206–211.
Singh, W. M. & Dash, B. C. (1988). *Pesticides*, **22**, 33–37.
Spackman, M. A. & Jayatilaka, D. (2009). *CrystEngComm*, **11**, 19–32.
Stoe & Cie (2002). *X-AREA*, *X-RED32* and *X-SHAPE*. Stoe & Cie GmbH, Darmstadt, Germany.
Taggi, A. E., Hafez, A. M., Wack, H., Young, B., Ferraris, D. & Lectka, T. (2002). *J. Am. Chem. Soc.* **124**, 6626–6635.
Tenon, J. A., Carles, M. & Aycard, J.-P. (1995). *Acta Cryst.* C**51**, 2603–2606.
Turner, M. J., McKinnon, J. J., Wolff, S. K., Grimwood, D. J., Spackman, P. R., Jayatilaka, D. & Spackman, M. A. (2017). *Crystal Explorer 17*. The University of Western Australia.
Vančo, J., Švajlenová, O., Račanská, E. J., Muselík, J. & Valentová, J. (2004). *J. Trace Elem. Med. Biol.* **18**, 155–161.
Wozniak, K., He, H., Klinowski, J., Jones, W., Dziembowska, T. & Grech, E. (1995). *J. Chem. Soc. Faraday Trans.* **91**, 7–85.
Zheng, Y.-F. (2013). *Acta Cryst.* E**69**, o1349.

supporting information

Acta Cryst. (2020). E**76**, 1320-1324 [https://doi.org/10.1107/S2056989020009421]

Crystal structure, Hirshfeld surface analysis and DFT studies of (*E*)-2-{[(3-chloro-4-methylphenyl)imino]methyl}-4-methylphenol

Md. Serajul Haque Faizi, Emine Berrin Cinar, Alev Sema Aydin, Erbil Agar, Necmi Dege and Ashraf Mashrai

Computing details

Data collection: *X-AREA* (Stoe & Cie, 2002); cell refinement: *X-AREA* (Stoe & Cie, 2002); data reduction: *X-SHAPE* (Stoe & Cie, 2002); program(s) used to solve structure: *SHELXT2018/2* (Sheldrick, 2015a); program(s) used to refine structure: *SHELXL2018/3* (Sheldrick, 2015b); molecular graphics: *ORTEP-3 for Windows* (Farrugia, 2012), *XP* in *SHELXTL* (Sheldrick, 2008).

(*E*)-2-{[(3-Chloro-4-methylphenyl)imino]methyl}-4-methylphenol

Crystal data

$C_{15}H_{14}ClNO$
$M_r = 259.72$
Monoclinic, $P2_1/c$
$a = 8.0534$ (5) Å
$b = 6.3764$ (3) Å
$c = 25.3657$ (16) Å
$\beta = 96.392$ (5)°
$V = 1294.47$ (13) Å^3
$Z = 4$
$F(000) = 544$
$D_x = 1.333$ Mg m^{-3}
Mo $K\alpha$ radiation, $\lambda = 0.71073$ Å
Cell parameters from 9569 reflections
$\theta = 1.6$–30.3°
$\mu = 0.28$ mm^{-1}
$T = 296$ K
Stick, orange
0.65 × 0.37 × 0.21 mm

Data collection

Stoe IPDS 2 diffractometer
Radiation source: sealed X-ray tube, 12 x 0.4 mm long-fine focus
Plane graphite monochromator
Detector resolution: 6.67 pixels mm^{-1}
rotation method scans
Absorption correction: integration (X-RED32; Stoe & Cie, 2002)
$T_{min} = 0.885$, $T_{max} = 0.958$
7752 measured reflections
2414 independent reflections
1801 reflections with $I > 2\sigma(I)$
$R_{int} = 0.040$
$\theta_{max} = 25.5°$, $\theta_{min} = 1.6°$
$h = -9 \rightarrow 9$
$k = -7 \rightarrow 7$
$l = -30 \rightarrow 30$

Refinement

Refinement on F^2
Least-squares matrix: full
$R[F^2 > 2\sigma(F^2)] = 0.045$
$wR(F^2) = 0.137$
$S = 1.03$
2414 reflections
169 parameters
0 restraints
Hydrogen site location: mixed
H atoms treated by a mixture of independent and constrained refinement
$w = 1/[\sigma^2(F_o^2) + (0.0845P)^2 + 0.059P]$ where $P = (F_o^2 + 2F_c^2)/3$
$(\Delta/\sigma)_{max} < 0.001$
$\Delta\rho_{max} = 0.22$ e Å^{-3}
$\Delta\rho_{min} = -0.26$ e Å^{-3}

Special details

Geometry. All esds (except the esd in the dihedral angle between two l.s. planes) are estimated using the full covariance matrix. The cell esds are taken into account individually in the estimation of esds in distances, angles and torsion angles; correlations between esds in cell parameters are only used when they are defined by crystal symmetry. An approximate (isotropic) treatment of cell esds is used for estimating esds involving l.s. planes.

Fractional atomic coordinates and isotropic or equivalent isotropic displacement parameters (Å²)

	x	*y*	*z*	U_{iso}*/U_{eq}
Cl1	0.74526 (10)	0.21146 (12)	0.56404 (2)	0.0820 (3)
O1	0.3423 (3)	0.0128 (3)	0.32974 (7)	0.0729 (5)
N1	0.5050 (2)	0.3352 (3)	0.37421 (7)	0.0546 (4)
C9	0.3492 (2)	0.3538 (3)	0.28875 (8)	0.0495 (5)
C5	0.6021 (3)	0.4244 (3)	0.41869 (8)	0.0517 (5)
C10	0.2953 (3)	0.4790 (3)	0.24498 (8)	0.0532 (5)
H10	0.333321	0.616621	0.244352	0.064*
C6	0.6276 (3)	0.2994 (3)	0.46336 (8)	0.0558 (5)
H6	0.582700	0.164970	0.462883	0.067*
C8	0.4537 (3)	0.4436 (3)	0.33310 (8)	0.0540 (5)
H8	0.484407	0.583899	0.331729	0.065*
C7	0.7199 (3)	0.3742 (4)	0.50893 (8)	0.0560 (5)
C14	0.2942 (3)	0.1445 (3)	0.28904 (8)	0.0537 (5)
C11	0.1881 (3)	0.4072 (3)	0.20271 (8)	0.0544 (5)
C2	0.7902 (3)	0.5727 (4)	0.51180 (8)	0.0569 (5)
C3	0.7630 (3)	0.6946 (4)	0.46627 (9)	0.0624 (6)
H3	0.808124	0.828887	0.466715	0.075*
C4	0.6720 (3)	0.6247 (4)	0.42059 (9)	0.0606 (6)
H4	0.657040	0.711090	0.390901	0.073*
C12	0.1343 (3)	0.1995 (4)	0.20491 (9)	0.0603 (5)
H12	0.061070	0.146941	0.177099	0.072*
C13	0.1860 (3)	0.0705 (4)	0.24686 (9)	0.0618 (6)
H13	0.148288	−0.067273	0.246965	0.074*
C15	0.1266 (3)	0.5478 (4)	0.15702 (9)	0.0699 (7)
H15A	0.110835	0.687133	0.169929	0.105*
H15B	0.022293	0.495293	0.140088	0.105*
H15C	0.207326	0.550746	0.131900	0.105*
C1	0.8890 (3)	0.6569 (4)	0.56097 (9)	0.0722 (7)
H1A	0.817191	0.672248	0.588488	0.108*
H1B	0.935229	0.790941	0.553389	0.108*
H1C	0.977895	0.561373	0.572449	0.108*
H1	0.399 (4)	0.082 (5)	0.3505 (14)	0.099 (12)*

Atomic displacement parameters (Å²)

	U^{11}	U^{22}	U^{33}	U^{12}	U^{13}	U^{23}
Cl1	0.1001 (5)	0.0819 (5)	0.0596 (4)	0.0149 (4)	−0.0115 (3)	0.0193 (3)
O1	0.0944 (13)	0.0595 (10)	0.0617 (10)	−0.0062 (9)	−0.0051 (9)	0.0144 (8)
N1	0.0546 (10)	0.0596 (11)	0.0481 (9)	0.0028 (8)	−0.0013 (7)	0.0010 (8)

C9	0.0467 (11)	0.0521 (11)	0.0489 (11)	0.0015 (9)	0.0018 (8)	0.0018 (8)
C5	0.0497 (11)	0.0586 (12)	0.0458 (10)	0.0081 (9)	0.0014 (8)	0.0017 (8)
C10	0.0564 (12)	0.0506 (11)	0.0514 (11)	−0.0007 (9)	0.0007 (9)	0.0043 (9)
C6	0.0575 (12)	0.0535 (12)	0.0553 (11)	0.0105 (10)	0.0008 (9)	0.0040 (9)
C8	0.0542 (12)	0.0529 (12)	0.0528 (11)	0.0025 (9)	−0.0034 (9)	0.0023 (9)
C7	0.0569 (12)	0.0617 (13)	0.0481 (11)	0.0185 (10)	−0.0001 (9)	0.0050 (9)
C14	0.0601 (13)	0.0513 (11)	0.0496 (11)	0.0027 (10)	0.0062 (9)	0.0060 (9)
C11	0.0532 (12)	0.0616 (12)	0.0477 (11)	0.0017 (10)	0.0021 (9)	0.0008 (9)
C2	0.0531 (12)	0.0654 (14)	0.0510 (11)	0.0124 (10)	0.0010 (9)	−0.0064 (10)
C3	0.0648 (14)	0.0625 (14)	0.0583 (13)	−0.0030 (11)	0.0000 (10)	−0.0016 (10)
C4	0.0646 (13)	0.0642 (13)	0.0515 (11)	−0.0047 (11)	−0.0003 (10)	0.0060 (10)
C12	0.0586 (12)	0.0700 (14)	0.0507 (11)	−0.0053 (11)	−0.0003 (9)	−0.0081 (10)
C13	0.0692 (14)	0.0540 (12)	0.0621 (13)	−0.0097 (11)	0.0067 (11)	−0.0030 (10)
C15	0.0756 (16)	0.0780 (17)	0.0524 (12)	0.0013 (13)	−0.0093 (11)	0.0077 (11)
C1	0.0725 (15)	0.0864 (18)	0.0545 (13)	0.0117 (13)	−0.0067 (11)	−0.0140 (12)

Geometric parameters (Å, º)

Cl1—C7	1.735 (2)	C11—C12	1.397 (3)
O1—C14	1.354 (2)	C11—C15	1.505 (3)
O1—H1	0.79 (4)	C2—C3	1.389 (3)
N1—C8	1.281 (3)	C2—C1	1.502 (3)
N1—C5	1.418 (3)	C3—C4	1.374 (3)
C9—C10	1.397 (3)	C3—H3	0.9300
C9—C14	1.406 (3)	C4—H4	0.9300
C9—C8	1.446 (3)	C12—C13	1.372 (3)
C5—C6	1.382 (3)	C12—H12	0.9300
C5—C4	1.394 (3)	C13—H13	0.9300
C10—C11	1.378 (3)	C15—H15A	0.9600
C10—H10	0.9300	C15—H15B	0.9600
C6—C7	1.388 (3)	C15—H15C	0.9600
C6—H6	0.9300	C1—H1A	0.9600
C8—H8	0.9300	C1—H1B	0.9600
C7—C2	1.385 (3)	C1—H1C	0.9600
C14—C13	1.385 (3)		
C14—O1—H1	105 (2)	C7—C2—C1	123.1 (2)
C8—N1—C5	122.08 (19)	C3—C2—C1	120.7 (2)
C10—C9—C14	118.46 (18)	C4—C3—C2	122.6 (2)
C10—C9—C8	119.64 (19)	C4—C3—H3	118.7
C14—C9—C8	121.86 (18)	C2—C3—H3	118.7
C6—C5—C4	118.5 (2)	C3—C4—C5	120.1 (2)
C6—C5—N1	116.1 (2)	C3—C4—H4	120.0
C4—C5—N1	125.41 (19)	C5—C4—H4	120.0
C11—C10—C9	122.7 (2)	C13—C12—C11	122.0 (2)
C11—C10—H10	118.6	C13—C12—H12	119.0
C9—C10—H10	118.6	C11—C12—H12	119.0
C5—C6—C7	120.1 (2)	C12—C13—C14	120.4 (2)

C5—C6—H6	119.9	C12—C13—H13	119.8
C7—C6—H6	119.9	C14—C13—H13	119.8
N1—C8—C9	121.82 (19)	C11—C15—H15A	109.5
N1—C8—H8	119.1	C11—C15—H15B	109.5
C9—C8—H8	119.1	H15A—C15—H15B	109.5
C2—C7—C6	122.4 (2)	C11—C15—H15C	109.5
C2—C7—Cl1	119.58 (17)	H15A—C15—H15C	109.5
C6—C7—Cl1	118.04 (18)	H15B—C15—H15C	109.5
O1—C14—C13	118.7 (2)	C2—C1—H1A	109.5
O1—C14—C9	121.97 (19)	C2—C1—H1B	109.5
C13—C14—C9	119.36 (19)	H1A—C1—H1B	109.5
C10—C11—C12	117.03 (19)	C2—C1—H1C	109.5
C10—C11—C15	121.7 (2)	H1A—C1—H1C	109.5
C12—C11—C15	121.2 (2)	H1B—C1—H1C	109.5
C7—C2—C3	116.2 (2)		

C8—N1—C5—C6	170.44 (19)	C9—C10—C11—C15	177.6 (2)
C8—N1—C5—C4	−9.5 (3)	C6—C7—C2—C3	0.1 (3)
C14—C9—C10—C11	1.3 (3)	Cl1—C7—C2—C3	−179.31 (17)
C8—C9—C10—C11	−176.3 (2)	C6—C7—C2—C1	179.4 (2)
C4—C5—C6—C7	0.4 (3)	Cl1—C7—C2—C1	0.0 (3)
N1—C5—C6—C7	−179.51 (18)	C7—C2—C3—C4	−0.1 (3)
C5—N1—C8—C9	−177.49 (18)	C1—C2—C3—C4	−179.4 (2)
C10—C9—C8—N1	179.5 (2)	C2—C3—C4—C5	0.2 (4)
C14—C9—C8—N1	2.0 (3)	C6—C5—C4—C3	−0.4 (3)
C5—C6—C7—C2	−0.3 (3)	N1—C5—C4—C3	179.5 (2)
C5—C6—C7—Cl1	179.12 (16)	C10—C11—C12—C13	−0.6 (3)
C10—C9—C14—O1	179.3 (2)	C15—C11—C12—C13	−178.4 (2)
C8—C9—C14—O1	−3.1 (3)	C11—C12—C13—C14	0.4 (4)
C10—C9—C14—C13	−1.5 (3)	O1—C14—C13—C12	179.9 (2)
C8—C9—C14—C13	176.1 (2)	C9—C14—C13—C12	0.6 (3)
C9—C10—C11—C12	−0.3 (3)		

Hydrogen-bond geometry (Å, º)

*Cg*1 is the centroid of the C2–C7 ring.

D—H···*A*	*D*—H	H···*A*	*D*···*A*	*D*—H···*A*
O1—H1···N1	0.79 (4)	1.89 (3)	2.625 (3)	153 (3)
C1—H1*C*···Cl1	0.96	2.91	3.072 (3)	91
C1—H1*A*···N1^{i}	0.96	2.86	3.734 (3)	152
C1—H1*C*···*Cg*1^{ii}	0.96	2.92	3.617 (2)	131

Symmetry codes: (i) −*x*+1, −*y*+1, −*z*+1; (ii) −*x*, −*y*+2, −*z*.